DOI: 10.1002/ejic.200801062

Novel Gallium Complexes with Malonic Diester Anions as Molecular Precursors for the MOCVD of Ga_2O_3 Thin Films

Malte Hellwig,[a] Ke Xu,[a] Davide Barreca,[b] Alberto Gasparotto,[c] Manuela Winter,[a] Eugenio Tondello,[c] Roland A. Fischer,[a] and Anjana Devi*[a]

Keywords: Gallium / Chemical vapor deposition / Thin films / Oxides / O ligands

Five different homoleptic gallium complexes with malonic diester anions [Ga(ROCOCHOCOR)$_3$] [R = Me (**1**), Et (**2**), *i*Pr (**3**), *t*Bu (**4**) and $SiMe_3$ (**5**)] have been synthesised and characterised by ^1H and ^{13}C NMR, IR spectroscopy, electron ionisation mass spectrometry (EI-MS), and single-crystal X-ray diffraction. The thermal properties of the obtained compounds were evaluated by thermogravimetric studies to assess their suitability as precursors for the metal-organic chemical vapour deposition (MOCVD) of Ga_2O_3 thin films. MOCVD of Ga_2O_3 thin films was carried out starting from compound **2** in light of the promising features of this precursor. The as-deposited layers are amorphous and can be transformed into the monoclinic β-Ga_2O_3 phase upon annealing at 1000 °C ex situ. The film morphology was studied by scanning electron microscopy (SEM), and its composition was investigated by energy-dispersive X-ray spectroscopy (EDXS) and X-ray photoelectron spectroscopy (XPS). Almost stoichiometric Ga_2O_3 thin films with low levels of carbon incorporation were obtained.

Introduction

Gallium oxide (β-Ga_2O_3) is a wide-bandgap material (ca. 4.9 eV)[1] with good chemical and thermal stability that is known to exhibit interesting electrical[2,3] and luminescence properties.[4,5] Recent renewed interest in this compound has arisen since it is a transparent conducting oxide (TCO) and shows promising features for applications in the field of optoelectronics.[6,7] Other uses include the development of gas-sensing devices for both oxygen[8–11] and reducing gases.[12,13] Furthermore, an insulator-to-metal transition with a relevant conductivity variation has recently been observed in amorphous gallium oxide thin films.[14]

Several physical and chemical techniques, such as sputtering,[15,16] electron-beam evaporation,[17] molecular-beam epitaxy (MBE),[18,19] pulsed-laser deposition (PLD),[20,21] sol-gel,[22] spray pyrolysis,[23] MOCVD[24–26] and atomic-layer deposition (ALD),[27,28] have been employed to deposit Ga_2O_3 coatings. The latter two are promising chemical approaches due to their inherent versatility, their good step coverage over complex device geometries and the possibility of achieving uniform large-area depositions. To date, the major limitation in the MOCVD of Ga_2O_3 has been the availability of suitable Ga precursors. In fact, the primary challenge in the chemistry of these complexes is the coordinative saturation and stabilisation of the Lewis acidic metal centre, which is essential to prevent oligomerisation and consequent detrimental volatility losses. $GaCl_3$, which is dimeric in the solid state, has been used for the CVD of gallium oxide,[11] although its chief drawback is the possible incorporation of chlorine. Another widely used precursor is trimethylgallium [Ga(CH$_3$)$_3$],[29,30] which, despite its high volatility, presents difficulties in handling due to its pyrophoric nature.

Different strategies have been employed in recent years to develop novel improved precursors for the MOCVD of Ga_2O_3 thin films. To this end, the substitution of one or more methyl groups in Ga(CH$_3$)$_3$ with alcohols led to more stable complexes.[31,32] In the case of gallium alkoxides [Ga(OR)$_3$]$_x$, which are reported to be tetramers for R = Me, Et, *n*Bu,[33] an increase in the steric demand of the alkoxide ligands (R = *i*Pr, *t*Bu) leads to more volatile dimeric species.[34,35] Improved precursors can also be obtained by introducing functionalised groups capable of electronic and/or steric stabilisation of the metal centre.[36] The use of monomeric group-13 sesquialkoxides has also been reported, although these complexes possess poor thermal properties.[37] A recent report has described the growth of Ga_2O_3 thin films by aerosol-assisted CVD (AA-CVD) by using gallium amides and donor-functionalised alcohols.[38] Another common choice has been the use of chelating ligands like β-diketonates, although known homoleptic gallium β-diketonate complexes such as Ga(acac)$_3$, Ga(dbm)$_3$ and

[a] Inorganic Materials Chemistry, Lehrstuhl für Anorganische Chemie II, Ruhr-Universität Bochum,
44780 Bochum, Germany
E-mail: anjana.devi@rub.de
[b] ISTM-CNR and INSTM – Department of Chemistry, Padova University,
35131 Padova, Italy
[c] Department of Chemistry – Padova University and INSTM,
35131 Padova, Italy

$Ga(thd)_3$ [acac = 2,4-pentanedionate; dbm = 1,3-diphenylpropane-1,3-dionate (dibenzoylmethane); thd = 2,2,6,6-tetramethyl-3,5-heptanedionate] exhibit high melting points and low volatility.[39,40]

In the last few years we have successfully developed promising precursors of various metals with chelating ligands such as β-oxo esters and malonates.[41–44] The presence of an ester group in the ligand skeleton offers important advantages for both the stabilisation of electrophilic metal centres by π-electron donation and for triggering low-temperature MOCVD decomposition by the introduction of a potential cleavage site in the molecule. The present work focuses on the development of MOCVD precursors for Ga_2O_3 thin films by using malonates as chelating ligands. Such moieties are expected to lead to all-oxygen, coordinatively saturated Ga complexes, as in the case of β-diketonates. The final goal is the easy obtainment of Ga precursors, which are volatile and stable to both air and moisture. Herein we report the synthesis and characterisation of novel homoleptic gallium malonates, where the terminal group in the ligand skeleton is systematically varied, and an investigation of the effect of this variation on the volatility and thermal characteristics of the resulting compounds. Five gallium complexes with malonic diester anions were synthesised: $[Ga(dMeml)_3]$ (**1**), $[Ga(dEtml)_3]$ (**2**), $[Ga(di\text{Prml})_3]$ (**3**), $[Ga(dbml)_3]$ (**4**), $[Ga(dtmsml)_3]$ (**5**) [dMeml, dEtml, di*P*rml, dbml, dtmsml = dimethyl, diethyl, diisopropyl, di-*tert*-butyl, bis(trimethylsilyl) malonate anion, respectively]. The most promising precursor in terms of thermal properties (**2**) was evaluated for the MOCVD of Ga_2O_3, and the preliminary results on film growth are also presented and discussed.

Results and Discussion

(i) Synthesis of the Gallium Complexes with Malonic Diester Anions

The homoleptic gallium complexes **1**–**5** were synthesised by a salt metathesis route, whereby a solution of $GaCl_3$ in diethyl ether was added to a freshly prepared suspension of the lithiated malonic diester ligand (1:3 ratio). Compounds **1**–**5** were obtained as solids after recrystallisation from hexane and were found to be highly soluble in hexane and toluene. The spectroscopic and analytical data for compounds **1**–**5** indicate that they are all monomeric. The crystallographic data for all these compounds can be found in the Experimental Section. Since all the synthesised complexes possess almost identical structural features, only two of them, namely $[Ga(dEtml)_3]$ (**2**) and $[Ga(dtmsml)_3]$ (**5**), are described in detail as representative examples (Figure 1).

In each case the Ga^{III} centre is homoleptically coordinated by three chelating malonic diester anion ligands, which results in a slightly distorted octahedral environment. This geometry is evidenced from the bite angle as well as the *cis* and *trans* angles observed in these complexes, which differ only slightly from ideal octahedral values [O1–Ga1–O2 92.35° (**2**)/O1–Ga1–O2 89.05° (**5**); O2–Ga1–O5′ 177.11°

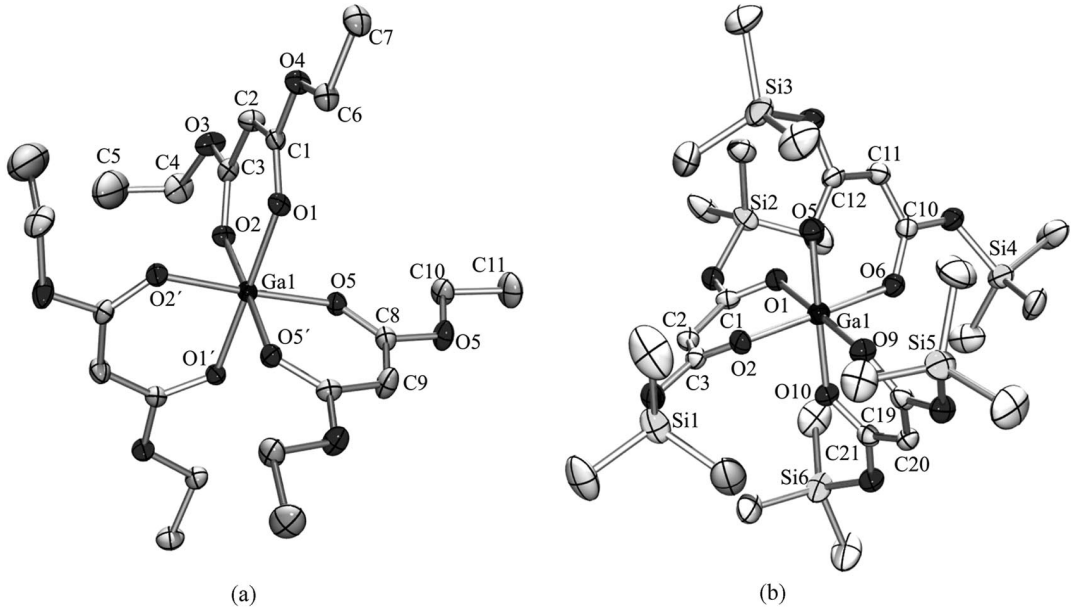

Figure 1. Molecular solid-state structure of (a) $Ga(dEtml)_3$ (**2**) and (b) $Ga(dtmsml)_3$ (**5**) (ORTEP, thermal ellipsoids shown at the 50% level; hydrogen atoms are omitted for clarity). Selected bond lengths [Å] and angles [°] for **2**: Ga1–O1 1.955(2), Ga1–O2 1.948(2), Ga1–O5 1.950(2); O2–Ga1–O1 92.35(7), O2–Ga1–O5 88.78(8), O5–Ga1–O1 90.02(7), O5′–Ga1–O5 91.17(10), O2–Ga1–O5′ 177.117, O1–Ga1–O1′ 179.20(10). Selected bond lengths [Å] and angles [°] for **5**: Ga1–O1 1.969(3), Ga1–O5 1.941(3), Ga1–O9 1.943(3); O1–Ga1–O2 89.05(11), O5–Ga1–O9 90.54(12), O10–Ga1–O1 89.14(11), O6–Ga1–O1 88.98(12), O5–Ga1–O10 178.55(12), O9–Ga1–O1 178.69(12). Symmetry-equivalent atoms (–*x*, *y*, 0.5 – *z*) are labeled as primed atoms.

(**2**)/O9–Ga1–O1 178.69° (**5**)]. These values are in good agreement with those for other gallium β-diketonate complexes such as [Ga(acac)$_3$] (O–Ga–O$_{bite}$ 91.3–92.2°; O–Ga–O$_{cis}$ 88.0–91.1°; O–Ga–O$_{trans}$ 177.8–179.7°).[45] The Ga–O bond lengths, which differ slightly in the two complexes (1.948–1.955 Å for **2** and 1.941–1.969 Å for **5**), are similar to those observed in other gallium β-diketonates {average Ga–O bond length in [Ga(acac)$_3$]: 1.952 Å, in [Ga(hfac)$_3$]: 1.954 Å (hfac = 1,1,1,5,5,5-hexafluoro-2,4-pentanedionate)}.[39,45]

Interestingly, the GaO_2C_3 metallacycles in all complexes deviate from planarity. Thus, the angles of the intersecting GaO_2 and C_3 planes are in the range 1.13–2.92° in **2** and 22.34–24.25° in **5**, possibly due to steric repulsions in the ligand sphere.

The monomeric structure of complexes **1**–**5** was further confirmed by ^{1}H and ^{13}C NMR spectra recorded in C_6D_6 at room temperature. In the case of **2**, the resulting ^{1}H NMR spectra appear more complex due to the diastereotopic nature of the ethyl CH_2 group, which generates a higher order spin system and results in a multiplet centred at δ = 4.08 ppm (see Experimental Section). The ethyl CH_3 protons and the proton of the central carbon atom of the ester backbone are observed as a triplet and a singlet at δ = 1.00 and 5.13 ppm, respectively.

The IR spectra of all compounds were recorded in the range 3500–400 cm^{-1}. The observed bands near 3000 cm^{-1} can be attributed to the C–H stretching modes. Tentative assignments of the IR absorption frequencies are based on previously characterised compounds having similar key structures.[39,40,46,47] Strong bands are observed in the carbonyl region (1581–1605 cm^{-1}), and metal–oxygen bands are located in the lower frequency region (450–500 cm^{-1}). The characteristic C=O, C=C and Ga–O stretching vibrations of compounds **1**–**5** are summarised in Table 1.

The EI mass spectra for gallium complexes **1**–**5** provide information regarding the fragmentation pathways of the compounds under gas-phase ionisation conditions. Although such studies have been used previously to predict possible mechanisms for CVD processes,[48] care must be taken when extrapolating information obtained from mass spectra to the CVD environment since the latter is thermally induced and the processing conditions are rather different.[49] Based on the obtained data, however, two general fragmentation pathways are proposed. Thus, whereas the splitting of one or multiple ester ligands could be observed for all five complexes, the detected fragments from **3** and **4** (Scheme 1) were attributed to the McLafferty rearrangement, which is typical for esters.[41–44,50–52]

Table 1. Comparison of selected stretching vibrations for compounds **1**–**5** with those reported for other gallium β-diketonate complexes.

	ν(C=O) [cm^{-1}]	ν(C=C) [cm^{-1}]	ν(Ga–O) [cm^{-1}]
[Ga(dMeml)$_3$] (**1**)	1605	1507	462
[Ga(dEtml)$_3$] (**2**)	1604	1509	499
[Ga(d*i*Prml)$_3$] (**3**)	1597	1502	457
[Ga(dbml)$_3$] (**4**)	1595	1501.	471
[Ga(dtmsml)$_3$] (**5**)	1581	n.a.	456
[Ga(acac)$_3$][46,47]	1600	1550	446
[Ga(thd)$_3$][39]	1569	1539	482

Since complex **4** exhibits both fragmentation pathways, the proposed mechanism is explained on the basis of this example (Scheme 1). The molecular ion peak of **4** is detected at *m*/*z* (%) = 714 (5). The first fragmentation corresponds to the sequential loss of three isobutene molecules as a consequence of the McLafferty rearrangement {*m*/*z* (%) = 658 (25) [M$^+$ – C$_4$H$_8$], 602 (5) [M$^+$ – 2 C$_4$H$_8$], 546 (5) [M$^+$ – 3 C$_4$H$_8$]}. The peak at *m*/*z* (%) = 499 (25) can be assigned to the loss of an entire dbml ligand. The resulting fragment, in turn, undergoes four sequential McLafferty rearrangements, which results in the peaks at *m*/*z* = 443, 387, 331 and 275. The base peak is located at *m*/*z* = 56 and corresponds to isobutene. The absence of peaks at *m*/*z* values higher than the molecular ion suggests a monomeric structure, in agreement with the above observations.

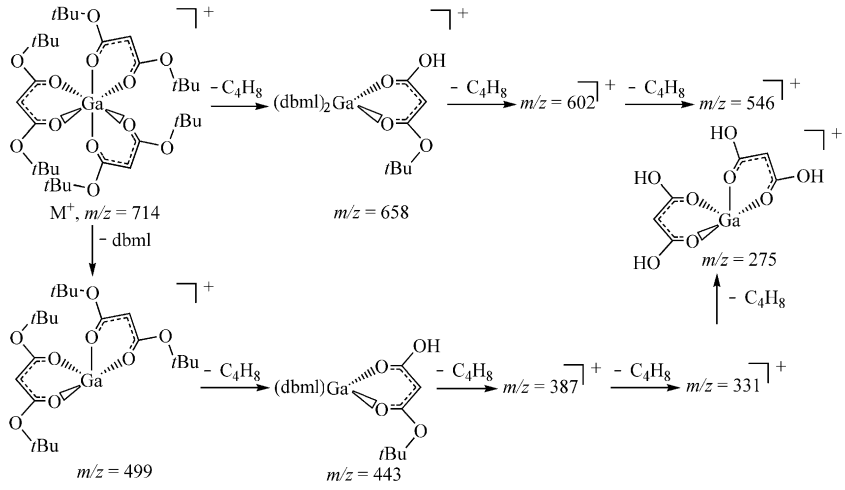

Scheme 1. Proposed EI-MS fragmentation scheme for compound **4**.

(ii) Thermal Properties

One of the main aims of this work was to evaluate the suitability of these complexes for MOCVD, with particular attention being paid to their thermal properties, therefore a preliminary characterisation was performed by measuring the melting points in sealed capillaries. Compounds **1**–**3** melt between 102 and 135 °C, which are very promising values when compared to gallium β-diketonate analogues, which melt at significantly higher temperatures {[$Ga(acac)_3$]: 192–194 °C;[53] [$Ga(thd)_3$]: 220 °C;[39] [$Ga(dbm)_3$]: 284 °C}.[40]

The volatility and decomposition characteristics of all complexes were analysed by thermogravimetry (TG). The temperature window between volatilisation and decomposition is very narrow for complexes **4** and **5**, thus indicating their unsuitability for thermal MOCVD. Figure 2a shows the TG curves for compounds **1**–**3**.

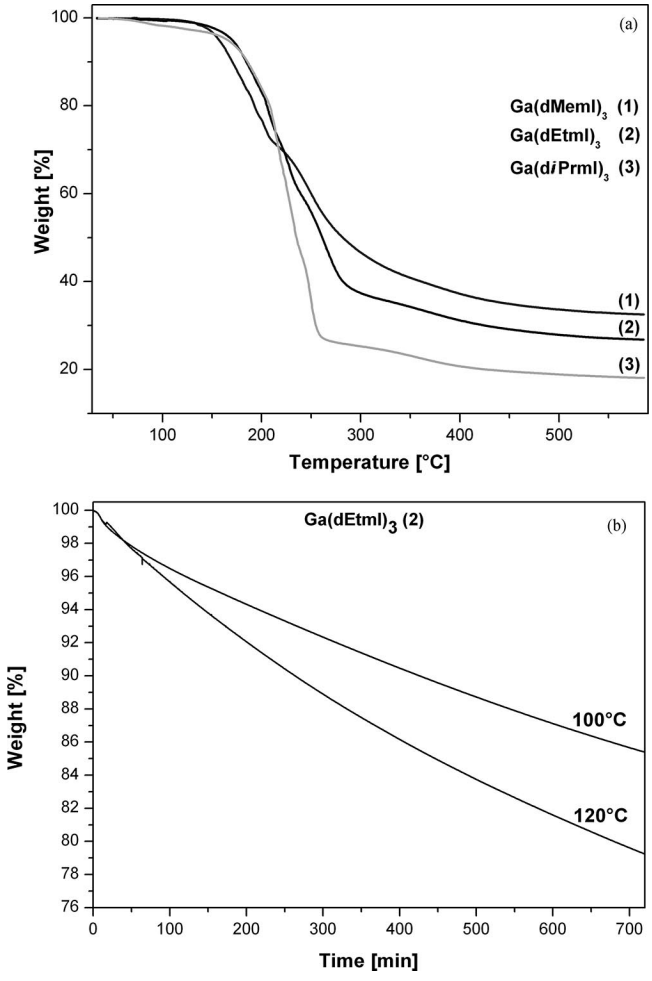

Figure 2. (a) TG curves for **1**–**3** recorded at a heating rate of 3 °C min^{-1} and a nitrogen flow of 300 mL min^{-1}. (b) Isothermal studies of **2** performed at 100 and 120 °C.

The temperature onset of volatilisation for these compounds ranges from 50 to 120 °C. Compound **2** has the lowest onset temperature of volatilisation (around 50 °C). Above 200 °C, the shoulders observed in the TG curves indicate that the compound begins to decompose. Residual weights corresponding to 32.5%, 26.8% and 18.1% for compounds **1**–**3**, respectively, were obtained at temperatures above 300 °C.

It is worthwhile underlining that the decomposition onset temperature is much lower than those of classical Ga β-diketonate complexes such as [$Ga(acac)_3$] (280 °C) or [$Ga(thd)_3$] (360 °C). This phenomenon could be due to the presence of additional cleavage sites (oxo ester groups in the ester ligand) in the present molecular precursors, which can advantageously facilitate lower temperature film deposition. The TG studies suggest that compounds **1**–**3** have a sufficiently large temperature window between volatilisation and decomposition for use as MOCVD precursors and that they are more volatile than classical Ga β-diketonates. Compound **2** was found to be the most volatile, as it sublimes at lower temperatures and has the lowest melting point (102 °C) of all the complexes herein reported. Isothermal studies carried out on compound **2** at two different temperatures are shown in Figure 2b. As can be observed, the precursor sublimes at constant rates for long periods of time. The sublimation rates were determined to be 1.56×10^{-3} and 1.85×10^{-3} mg min^{-1} at 100 and 120 °C, respectively. The almost linear trends in the isothermal TG curves are indicative of clean vaporisation processes, with no clear signs of premature decomposition. These results imply that a constant and reproducible precursor vapour supply can be expected in MOCVD applications.

(iii) MOCVD of Ga_2O_3 Thin Films by Using [$Ga(dEtml)_3$] (2)

Based on its more promising thermal properties, compound **2** was selected to deposit Ga_2O_3 thin films. In agreement with the results obtained by thermal analysis, this complex could be efficiently vaporised at temperatures as low as 110 °C. In comparison, when using [$Ga(acac)_3$] in the same system, vaporisation temperatures of 135 °C were necessary for Ga_2O_3 film growth.

Preliminary depositions from compound **2** were carried out on Si(100) substrates in the temperature range 400–800 °C by using oxygen as reactive gas. The films were optically shiny in appearance and adhered very well to the underlying substrate, as demonstrated by the scotch-tape test. The threshold temperature for film growth was 400 °C (film thickness 60 nm), whereas a maximum thickness of 260 nm was obtained at 700 °C (Figure 3) with a growth rate of 4.3 nm min^{-1}.

The film microstructure as a function of deposition temperature was analysed by XRD. Even at temperatures as high as 800 °C, the XRD pattern was featureless, except for the reflection from Si(200) located at 2θ = 33.17°, thereby indicating the amorphous nature of the films (Figure 4). Films deposited at 700 °C (the temperature corresponding to the maximum growth rate) were therefore subjected to post-deposition annealing at 1000 °C for 60 min in the presence of oxygen [100 sccm (sccm = standard cubic centimeters per minute)]. The resulting XRD pattern showed broad reflections which could be assigned to the monoclinic β-Ga_2O_3 phase (Figure 4).[54]

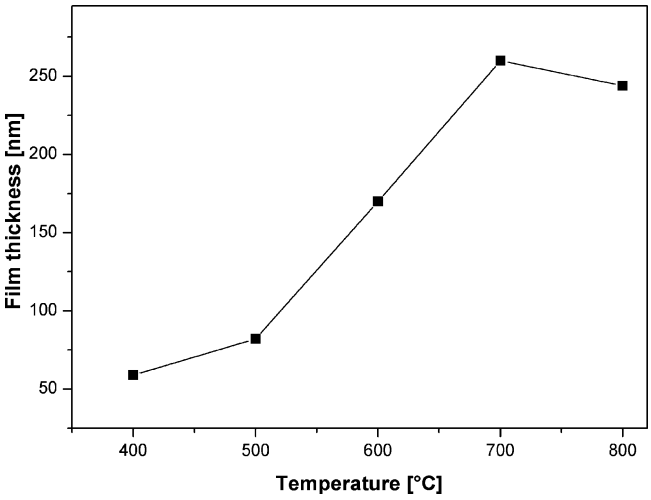

Figure 3. Growth rate vs. substrate temperature for gallium oxide thin films deposited on Si(100) substrates by using compound **2**.

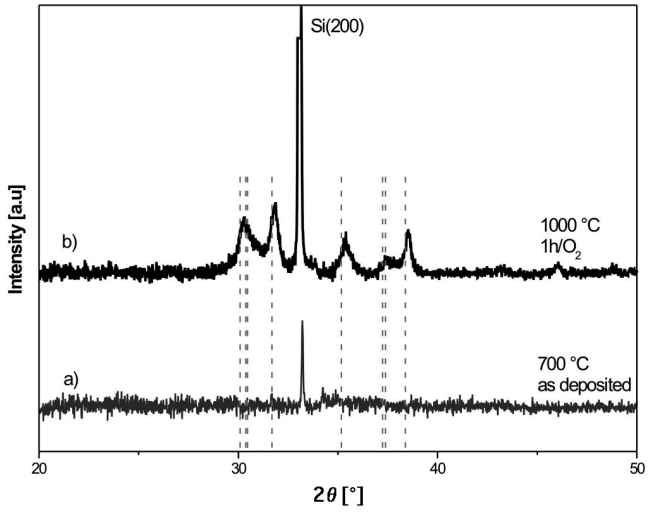

Figure 4. XRD patterns of an as-deposited (T = 700 °C) amorphous Ga_2O_3 film (a) and a post-deposition annealed Ga_2O_3 film (annealing temperature 1000 °C in the presence of oxygen (b). The dashed lines correspond to the monoclinic β-Ga_2O_3 phase.[53]

The surface morphology of the Ga_2O_3 films was analysed by SEM, which displayed a uniform and homogeneous texture along with an apparently dense cross-sectional structure (Figure 5). EDX measurements confirmed the presence of only Ga and O, apart from the Si peak due to the substrate used.

The film's chemical composition was further investigated by XPS (Figure 6). As a general rule, the surface analysis revealed the presence of Ga, O and C. The absence of silicon photopeaks indicated a uniform substrate coverage. The carbon amount was drastically reduced after mild Ar^+ erosion, thus indicating that the carbon is mainly due to atmospheric exposure. In this regard, it is worthwhile to note that the spectral features of the C photopeak indicate the predominance of adventitious carbon along with a minor contribution located at a binding energy (*BE*) of

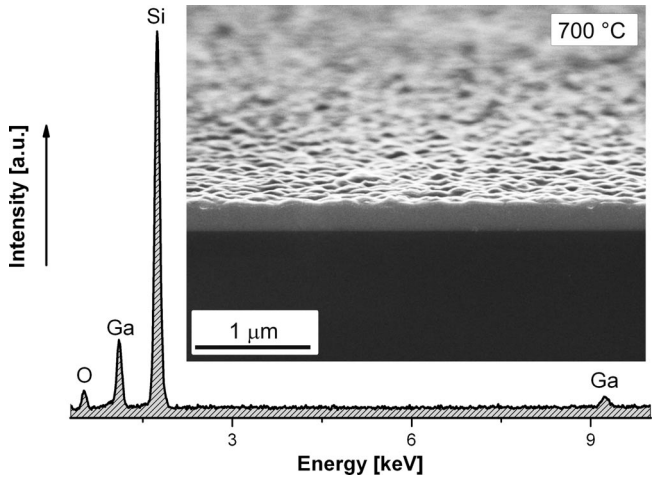

Figure 5. Representative cross-sectional SEM micrograph, and the corresponding EDX spectrum, of a Ga_2O_3 thin film deposited at 700 °C using compound **2**.

288.7 eV ascribed to the formation of gallium carbonates/hydrogencarbonates.[55] The intensity decrease experienced by this component upon Ar^+ erosion enabled us to attribute it to an interaction with atmospheric CO_2. Accordingly, the O and Ga surface atomic percentages were evaluated as 34.2 and 17.6 atom-%, respectively. The corresponding O/Ga ratio was found to be close to 1.9, a higher value than that expected for stoichiometric Ga_2O_3, in agreement with the features discussed for the C 1s signal. The O/Ga ratio was found to be lower (1.0) in the inner film regions than

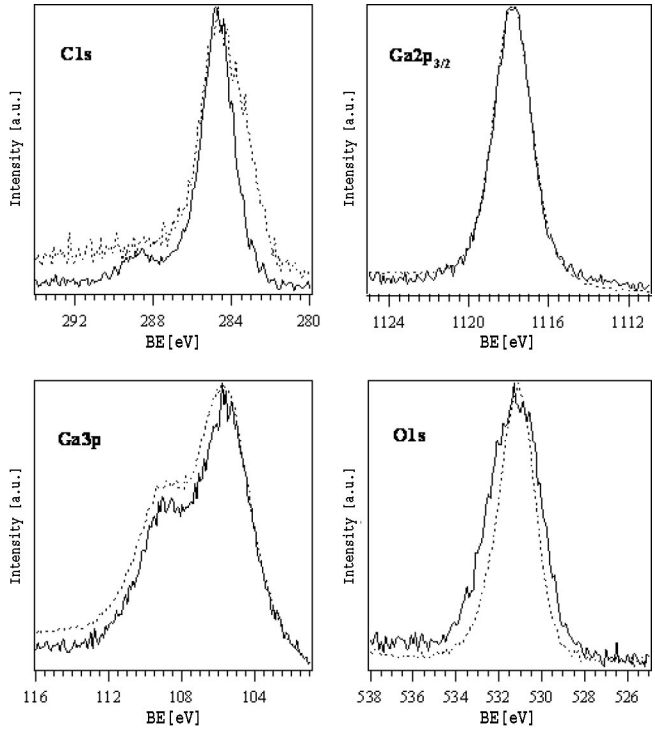

Figure 6. XPS photoelectron peaks of C 1s, Ga $2p_{3/2}$, Ga 3p and O 1s for a representative as-deposited Ga_2O_3 thin film grown at 600 °C from compound **2** before (continuous line) and after (dotted line) Ar^+ erosion for 10 min.

on the surface due to oxygen preferential sputtering, which is often observed upon XPS depth profiling of metal oxide films.[56]

Relevant Ga and O photoelectron peaks for a representative specimen grown from precursor **2** at 600 °C are displayed in Figure 6. The Ga $2p_{3/2}$ spectral features [*BE* = 1117.8 eV; full width at half maximum (*FWHM*) = 2.2 eV] agree well with the presence of Ga_2O_3 (Figure 6), the literature values for this oxide being found in the range 1116.9–1119.4 eV.[38,55,57,58] The Ga 3p line [*FWHM* = 5.2 eV, *BE*(Ga $3p_{3/2}$) = 105.6 eV] further confirmed the presence of Ga_2O_3 (literature values: 105.5–105.7 eV).[58]

The surface O 1s peak (*BE* = 531.2 eV, *FWHM* = 2.8 eV) was found in the range expected for Ga_2O_3.[38,59,60] The weak tailing towards high *BE*s could be due to the presence of surface hydroxy/carbonate species,[55] in accordance with the above discussed features. Upon erosion, the O 1s signal became narrower, thus indicating the almost complete disappearance of the high *BE* species in the inner sample layers.

Conclusions

This work represents the first literature report of the synthesis and characterisation of homoleptic gallium complexes with malonic diester anions [Ga(ROCOCHOCOR)$_3$] [R = Me (**1**), Et (**2**), *i*Pr (**3**), *t*Bu (**4**) and $SiMe_3$ (**5**)]. These compounds, all of which can readily be handled on the bench, are conveniently obtained by a simple and straightforward synthesis route, which is amenable to scale-up applications.

As a general rule, the Ga^{III} centre in the above complexes is coordinated by three chelating malonic diester anion ligands in an almost ideal octahedral geometry to give a monomeric structure, which is a very favourable feature in view of eventual MOCVD applications. The gallium complexes **1**–**3** in particular show significantly lower melting points than classical Ga^{III} β-diketonates. Thermogravimetric and isothermal measurements indicate that compound **2** possesses the highest sublimation rate. As a consequence, this precursor was selected for preliminary CVD depositions of gallium oxide films. The as-deposited samples remain amorphous up to a substrate temperature of 800 °C and undergo crystallisation into the monoclinic β-Ga_2O_3 phase only upon ex situ annealing at 1000 °C in the presence of oxygen. Compositional analyses have confirmed the synthesis of Ga_2O_3 films. As a whole, the present data highlight the potential of the proposed molecular compounds as innovative CVD precursors for Ga_2O_3 thin films.

Experimental Section

General Procedures: All reactions were performed in a conventional vacuum/argon line by using standard Schlenk techniques. Samples for analysis were prepared in an argon-filled glove box (MBraun). All solvents were dried and purified by an automatic solvent purification system attached directly to the glove box (MBraun solvent purification system) and stored over molecular sieves (4 Å). The NMR solvents were degassed and dried with activated molecular sieves. Dimethyl malonate (HdMeml; Acros 99%), diethyl malonate (HdEtml; Acros99%), diisopropyl malonate (Hd*i*Prml; Aldrich 99%), di-*tert*-butyl malonate (Hdbml; Fluka >98%) and bis(trimethylsilyl) malonate (Hdtmsml; Fluka >98%) were used as received. The lithiated diesters Li(dRml) were prepared by adding *n*BuLi (2.5 M in hexane) to the diesters in hexane at 0 °C. High-purity $GaCl_3$ (99.999%) was purchased from ABCR and used without further purification. Elemental analyses were performed by using a CHNSO Vario EL instrument. Melting points were measured in sealed capillaries under Ar. The IR spectra were recorded with a Bruker Alpha-T FTIR infrared spectrometer in transmission mode by using KBr pellets (200 mg of KBr/20 mg of substance). ^{1}H and ^{13}C NMR spectra were recorded with a Bruker Avance DPX 250 spectrometer. Electron impact (EI) mass spectra were recorded with a Varian MAT spectrometer at an ionizing energy of 70 eV. Thermogravimetric analyses (TGA) were performed by using a Seiko TG/DTA 6300S11 instrument (sample weight approx. 10 mg) at a heating rate of 3 °C min^{-1}. All measurements were performed at atmospheric pressure in the temperature range 30–600 °C under flowing N_2 (99.9999%; flow rate = 300 mL min^{-1}). For isothermal studies, approximately 8 mg of precursor was heated to a fixed temperature and maintained at that temperature under flowing N_2 for 12 h.

Synthesis of Gallium Complexes

[Ga(dMeml)$_3$] (1): A solution of $GaCl_3$ (0.53 g, 3 mmol) in diethyl ether (50 mL) was added dropwise to a freshly prepared suspension of Li(dMeml) in hexane, prepared from HdMeml (1.03 mL, 0.89 g, 9 mmol) at 0 C. The mixture was warmed to room temperature overnight. After refluxing for 4 h, the solvent was removed under vacuum. Extraction of the crude product with hexane (50 mL) and filtration through Celite led to a pale yellow solution. The solution was concentrated and cooled to –20 °C to give the product as colourless crystals. Yield (based on $GaCl_3$): 0.93 g (2.0 mmol, approx. 67%). M.p. 128 °C. $C_{15}H_{21}GaO_{12}$ (463.04): calcd. C 38.88, H 4.54; found C 38.19, H 4.11. EI-MS (70eV): *m*/*z* (%) = 462 (10) [M$^+$], 331 (30) [M$^+$ – dMeml], 200 (5) [M$^+$ – 2 dMeml], 101 (100) [dMeml – 2 CH_3]. ^{1}H NMR (250 MHz, C_6D_6, room temp.): δ = 4.98 [s, 3 H, GaOC(OCH$_3$)C*H*], 3.41 [s, 18 H, GaOC(OC*H*$_3$)CH] ppm. ^{13}C NMR (250 MHz, C_6D_6, room temp.): δ = 176.69 [GaO*C*-(OCH$_3$)CH], 66.85 [GaOC-(OCH$_3$)*C*H], 51.62 [GaOC(O*C*H$_3$)CH] ppm. IR: $\tilde{\nu}$ = 1605 (s), 1507 (s), 1449 (s), 1411 (m), 1319 (s), 1190 (s), 1152 (s), 1083 (s), 1017 (m), 988 (m), 907 (w), 785 (s), 717 (m), 548 (w), 462 (s), 385 (w) cm^{-1}.

Compounds **2**–**5** were prepared in a similar manner to compound **1**.

[Ga(dEtml)$_3$] (2): Yield (based on $GaCl_3$): 1.21 g (2.22 mmol, approx. 74%). M.p. 102 °C. $C_{21}H_{33}GaO_{12}$ (547.19): calcd. C 46.09, H 6.08; found C 45.73, H 6.66. EI-MS (70eV): *m*/*z* (%) = 546.12 (15) [M$^+$], 387 (100) [M$^+$ – dEtml], 229 (10) [M$^+$ – 2 dEtml], 159 (5) [dEtml]. ^{1}H NMR (250 MHz, C_6D_6, room temp.): δ = 5.13 [s, 3 H, GaO(COCH$_3$)C*H*], 4.08 [m, 12 H, GaOC(OCC*H*$_2$CH$_3$)CH], 1.00 [t, $^3J_{H,H}$ = 7.1 Hz, 24 H, GaOC(OCCH$_2$C*H*$_3$)CH]. ^{13}C NMR (250 MHz, C_6D_6, room temp.): δ = 176.38 [GaO*C*(OCH$_2$CH$_3$)CH], 67.35 [GaOC(OCH$_2$CH$_3$)*C*H], 60.77 [GaOC(O*C*H$_2$CH$_3$)CH], 14.54 [GaOC(OCH$_2$*C*H$_3$)CH] ppm. IR: $\tilde{\nu}$ = 1604 (s), 1509 (s), 1486 (s), 1387 (s), 1310 (s), 1152 (s), 1081 (s), 1008 (m), 903 (w), 826 (w), 783 (s), 714 (m), 499 (m), 429 (m) cm^{-1}.

[Ga(d*i*Prml)$_3$] (3): Yield (based on $GaCl_3$): 1.06 g (1.68 mmol, approx. 56%). M.p. 135 °C. $C_{27}H_{45}GaO_{12}$ (631.35): calcd. C 51.35, H 7.18; found C 51.34, H 7.31. EI-MS (70eV): *m*/*z* (%) = 629 (10)

[M^+], 587 (2) [$M^+ - C_3H_7$], 442 (100) [M^+ – d*i*Prml], 400 (7) [M^+ – d*i*Prml – C_3H_7], 358 (5) [M^+ – d*i*Prml – 2 C_3H_7], 256 (15) [M^+ – 2 d*i*Prml], 43 (60) [C_3H_7]. ^{1}H NMR (250 MHz, C_6D_6, room temp.): δ = 5.13 {sept, $^3J_{H,H}$ = 6.2 Hz, 6 H, GaOC[OCCH_2(CH$_3$)$_2$CH]}, 5.02 {s, 3 H, GaO[COCH$_2$(CH$_3$)$_2$]C*H*}, 1.09 {d, $^3J_{H,H}$ = 6.2 Hz, 6 H, GaOC[OCCH$_2$(CH_3)$_2$CH]}, 1.18 {d, $^3J_{H,H}$ = 6.2 Hz, 6 H, GaOC[OCCH$_2$(CH_3)$_2$CH]} ppm. ^{13}C NMR (250 MHz, C_6D_6, room temp.): δ = 176.00 {GaO*C*[OCH$_2$(CH$_3$)$_2$CH]}, 68.15 {GaOC-[OCH$_2$(CH$_3$)$_2$*C*H]}, 68.01 {GaOC[O*C*H$_2$(CH$_3$)$_2$CH]}, 22.16 {GaOC[OCH$_2$(*C*H$_3$)$_2$CH]}, 22.06 {GaOC[OCH$_2$(*C*H$_3$)$_2$CH]} ppm. IR: $\tilde{\nu}$ = 1597 (s), 1502 (s), 1370 (s), 1330 (m), 1341 (m), 1308 (s), 1159 (s), 1113 (s), 1072 (s), 1014 (m), 936 (w), 906 (m), 783 (s), 719 (m), 525 (m), 457 (m), 429 (w) cm^{-1}.

[Ga(dbml)$_3$] (4): Yield (based on $GaCl_3$): 1.37 g (1.92 mmol, approx. 64%). $C_{33}H_{57}GaO_{12}$ (715.51): calcd. C 55.39, H 8.03; found C 55.17, H 7.73. EI-MS (70eV): *m*/*z* (%) = 714 (5) [M^+], 658 (25) [$M^+ - C_4H_8$], 602 (5) [$M^+ - 2\ C_4H_8$], 546 (5) [$M^+ - 3\ C_4H_8$], 499 (25) [M^+ – dbml], 443 (10) [M^+ – dbml – C_4H_8], 387 (25) [M^+ – dbml – 2 C_4H_8], 331 (20) [M^+ – dbml – 3 C_4H_8], 274 (55) [M^+ – dbml – 4 C_4H_8], 57 (100) [C_4H_8]. ^{1}H NMR (250 MHz, C_6D_6, room temp.): δ = 4.87 {s, 54 H, GaOC[OC(CH$_3$)$_3$C*H*}, 1.51 {s, 54 H, GaOC[OC(CH$_3$)$_3$C*H*]} ppm. ^{13}C NMR (250 MHz, C_6D_6, room temp.): δ = 176.29 {GaO*C*[OC(CH$_3$)$_3$CH]}, 79.97 {GaOC[O*C*-(CH$_3$)$_3$CH]}, 69.97 GaOC[OC(CH$_3$)$_3$*C*H], 29.01 {GaOC[OC(*C*H$_3$)$_3$-CH]} ppm. IR: $\tilde{\nu}$ = 1595 (s), 1501 (s), 1391 (s), 1365 (s), 1343 (s), 1253 (m), 1130 (s), 1076 (s), 1006 (m), 921 (w), 883 (w), 850 (m), 809 (w), 783 (s), 724 (m), 682 (s), 500 (m), 471 (m), 403 (w), 390 (w) cm^{-1}.

[Ga(dtmsml)$_3$] (5): Yield (based on $GaCl_3$): 1.71 g (2.11 mmol, approx. 70%). $C_{25}H_{45}GaO_{12}Si_6$ (775.87): calcd. C 39.94, H 7.08; found C 40.1, H 6.63. EI-MS (70eV): *m*/*z* (%) = 563 (100) [M^+ – dtmsml], 247 (13) [dtms], 73 (29) [$SiMe_3$]. ^{1}H NMR (250 MHz, C_6D_6, room temp.): δ = 4.97 [s, 3 H, GaOC(OSiMe$_3$)C*H*], 0.35 {s, 54 H, GaOC[OSi(CH_3)$_3$]CH} ppm. ^{13}C NMR (250 MHz, C_6D_6, room temp.): δ = 171.01 [GaO*C*(OSiMe$_3$)CH], 71.21 [GaOC(OSi-Me$_3$)*C*H], 0.41 [GaOC[OSi(*C*H$_3$)$_3$CH] ppm. IR: $\tilde{\nu}$ = 1581 [s (br.)], 1418 (m), 1374 (m), 1278 (m), 1261 (m), 1202 (w), 1159 (w), 959 (w), 848 (w), 798 (w), 739 (w), 634 (w), 456 (w) cm^{-1}.

X-ray Crystallography: Single crystals of compounds **1**–**5** were mounted on thin glass capillaries and then cooled to the data-collection temperature (113 K). Diffraction data were collected with an Oxford X-calibur 2 diffractometer by using graphite-monochromated Mo-K_α radiation (λ = 0.71073 Å). All structures were solved by direct methods by using the SHELXL-97® software package and refined by full-matrix least-squares methods based on F^2 with all observed reflections. Final agreement factors are listed in Table 2. CCDC-706559, -706560, -706561, -706562 and -706563 (for **1**–**5**, respectively) contain the supplementary crystallographic data for this paper. These data can be obtained free of charge from The Cambridge Crystallographic Data Centre via www.ccdc.cam.ac.uk/data_request/cif.

Ga_2O_3 Film Synthesis and Characterisation: A cold-wall horizontal MOCVD system[61] operating under reduced pressure was used for thin-film deposition. The depositions were carried out on *p*-type Si(100) substrates (1.5 × 1.5 cm^2). The substrates were ultrasonically cleaned in acetone, propanol, rinsed with de-ionized water, and finally dried with nitrogen prior to each experiment. High-purity nitrogen (99.9999%, flow rate 50 sccm) and oxygen (99.998%, flow rate 50 sccm) were used as the carrier and reactive gases, respectively, and their flow rates were controlled by using mass-flow controllers (MKS). In each deposition, around 100 mg of compound **2** was placed in a vaporiser maintained at 110 °C. The films were deposited at a total pressure of 5 mbar over the temperature range 400–800 °C for 60 min. XRD analysis of the films was carried out with a Bruker AXS D8 Avance diffractometer by using Cu-K_α radiation (1.5418 Å) with a position-sensitive detector (PSD, Bragg–Brentano geometry). The surface morphology and film thickness (from cross-sectional micrographs) was studied by SEM [LEO (Zeiss)]. An Oxford ISIS EDX system coupled to the SEM instrument was used for composition analysis. XPS spectra were recorded with a Perkin–Elmer Φ 5600ci spectrometer by using a monochromatized Al-K_α excitation source (1486.6 eV). The *BE* shifts were corrected by assigning a value of 284.8 eV to the C 1s line of adventitious carbon. The atomic compositions were evaluated by using sensitivity factors provided by the Φ V5.4A software. In order to obtain a more accurate evaluation of atomic percentages, the Ga 3p signal was used in the quantification instead of the more intense Ga 2p photopeak, due to its appreciable *BE* difference with respect to the O and C peaks. This feature would imply the analysis of photoelectrons with different escape depths,

Table 2. Crystallographic data for compounds **1**–**5**.[a]

	[Ga(dMeml)$_3$] (**1**)	[Ga(dEtml)$_3$] (**2**)	[Ga(d*i*Prml)$_3$] (**3**)	[Ga(dbml)$_3$] (**4**)	[Ga(dtmsml)$_3$] (**5**)
Empirical formula	$C_{15}H_{21}GaO_{12}$	$C_{21}H_{33}GaO_{12}$	$C_{54}H_{90}Ga_2O_{24}$	$C_{33}H_{57}GaO_{12}$	$C_{27}H_{57}GaO_{12}Si_6$
Formula mass	463.04	547.19	1262.70	715.51	811.99
Crystal size [mm]	0.30 × 0.25 × 0.20	0.35 × 0.30 × 0.20	0.38 × 0.30 × 0.25	0.23 × 0.18 × 0.15	0.32 × 0.25 × 0.20
Crystal system	monoclinic	monoclinic	triclinic	monoclinic	triclinic
Space group	*C*2/*c*	*C*2/*c*	$P\bar{1}$	$P2_1$	*P*1
a [Å]	24.1384(13)	17.8095(7)	11.5573(5)	10.5288(9)	11.017(2)
b [Å]	16.4985(5)	11.6190(3)	16.0787(7)	34.956(3)	11.184(2)
c [Å]	18.7042(7)	13.6769(3)	17.5854(5)	10.9359(5)	11.460(2)
α [°]	90	90	98.257(3)	90	111.98(3)
β [°]	125.080(3)	115.051(2)	90.281(3)	100.631(6)	107.34(3)
γ [°]	90	90	90.781(4)	90	106.94(3)
V [Å^3]	6095.8(4)	2563.91(13)	3233.6(2)	3955.8(5)	1112.9(4)
Z	12	4	2	4	1
$\rho_{calcd.}$ [g cm^{-3}]	1.514	1.418	1.297	1.201	1.212
Goodness-of-fit on F^2	0.879	1.074	0.981	1.016	0.976
Final *R* indices [$I > 2\sigma(I)$]	R_1 = 0.0297	R_1 = 0.0416	R_1 = 0.0718	R_1 = 0.0507	R_1 = 0.0451
	wR_2 = 0.0535	wR_2 = 0.1266	wR_2 = 0.1917	wR_2 = 0.0945	wR_2 = 0.1017
R indices (all data)	R_1 = 0.0720	R_1 = 0.0521	R_1 = 0.1281	R_1 = 0.0806	R_1 = 0.0561
	wR_2 = 0.0635	wR_2 = 0.1321	wR_2 = 0.2126	wR_2 = 0.1043	wR_2 = 0.1045

[a] $R_1 = \Sigma(||F_o| - |F_c||)/\Sigma|F_o|^{1/2}$. $wR_2 = [\Sigma w(F_o^2 - F_c^2)^2/\Sigma w(F_o^2)^2]^{1/2}$. $GOF = [\Sigma w(F_o^2 - F_c^2)^2/(N_o - N_p)]^{1/2}$.

thus yielding an uncorrected estimation.[56] Ar^+ sputtering was carried out at 3.5 kV and 0.5 mA cm^{-2} beam-current density, with an argon partial pressure of 5×10^{-8} mbar.

Acknowledgments

Financial support from the National Council of Research – Italian National Consortium for Materials Science and Technology – Molecular Design Department (CNR-INSTM PROMO) and Cassa di Risparmio di Padova e Rovigo (CARIPARO) Foundation within the project "Multi-layer optical devices based on inorganic and hybrid materials by innovative synthetic strategies" is acknowledged. The authors thank Dr. Harish Parala and Dr. Ramasamy Pothiraja for critically reviewing this manuscript.

[1] H. H. Tippins, *Phys. Rev.* **1965**, *140*, 316.
[2] M. R. Lorenz, J. F. Woods, R. J. Gambino, *J. Phys. Chem. Solids* **1967**, *28*, 403.
[3] T. Harwig, J. Schoonman, *J. Solid State Chem.* **1978**, *23*, 205.
[4] W. C. Herbert, H. B. Minnier, J. J. Brown Jr, *J. Electrochem. Soc.* **1969**, *116*, 1019.
[5] T. Harwig, F. Kellendonk, *J. Solid State Chem.* **1978**, *24*, 255.
[6] Z. Ji, J. Du, J. Fan, W. Wang, *Opt. Mater. (Amsterdam, Neth.)* **2006**, *28*, 415.
[7] M. Orita, H. Hiramatsu, H. Ohta, M. Hirano, H. Hosono, *Thin Solid Films* **2002**, *411*, 134.
[8] M. Fleischer, H. Meixner, *Sens. Actuators, B* **1991**, *4*, 437.
[9] M. Ogita, S. Yuasa, K. Kobayashi, Y. Yamada, Y. Nakanishi, Y. Hatanaka, *Appl. Surf. Sci.* **2003**, *212–213*, 397.
[10] M. Ogita, K. Higo, Y. Nakanishi, Y. Hatanaka, *Appl. Surf. Sci.* **2001**, *175–176*, 721.
[11] R. Binions, C. J. Carmalt, I. P. Parkin, *Meas. Sci. Technol.* **2007**, *18*, 190.
[12] T. Schwebel, M. Fleischer, H. Meixner, C. D. Kohl, *Sens. Actuators, B* **1998**, *49*, 46.
[13] M. Ogita, N. Saika, Y. Nakanishi, Y. Hatanaka, *Appl. Surf. Sci.* **1999**, *142*, 188.
[14] L. Nagarajan, R. A. De Souza, D. Samuelis, I. Valov, A. Boerger, J. Janek, K.-D. Becker, P. C. Schmidt, M. Martin, *Nat. Mater.* **2008**, *7*, 391.
[15] J. Frank, M. Fleischer, H. Meixner, *Sens. Actuators, B* **1996**, *B34*, 373.
[16] M. Rebien, W. Henrion, M. Hong, J. P. Mannaerts, M. Fleischer, *Appl. Phys. Lett.* **2002**, *81*, 250.
[17] N. C. Oldham, C. J. Hill, C. M. Garland, T. C. McGill, *J. Vac. Sci. Technol., A* **2002**, *20*, 809.
[18] Z. Yu, C. D. Overgaard, R. Droopad, M. Passlack, J. K. Abrokwah, *Appl. Phys. Lett.* **2003**, *82*, 2978.
[19] T. Oshima, N. Arai, N. Suzuki, S. Ohira, S. Fujita, *Thin Solid Films* **2008**, *516*, 5768.
[20] P. Wellenius, A. Suresh, J. F. Muth, *Appl. Phys. Lett.* **2008**, *92*, 021111/1.
[21] P. Gollakota, A. Dhawan, P. Wellenius, L. M. Lunardi, J. F. Muth, Y. N. Saripalli, H. Y. Peng, H. O. Everitt, *Appl. Phys. Lett.* **2006**, *88*, 221906/1.
[22] Y. Li, A. Trinchi, W. Wlodarski, K. Galatsis, K. Kalantar-Zadeh, *Sens. Actuators, B* **2003**, *B93*, 431.
[23] J. Hao, Z. Lou, I. Renaud, M. Cocivera, *Thin Solid Films* **2004**, *467*, 182.
[24] H. W. Kim, N. H. Kim, *J. Alloys Compd.* **2005**, *389*, 177.
[25] G. A. Battiston, R. Gerbasi, M. Porchia, R. Bertoncello, F. Caccavale, *Thin Solid Films* **1996**, *279*, 115.
[26] H. W. Kim, N. H. Kim, *Appl. Surf. Sci.* **2004**, *230*, 301.
[27] G. X. Liu, F. K. Shan, J. J. Park, W. J. Lee, G. H. Lee, I. S. Kim, B. C. Shin, S. G. Yoon, *J. Electroceram.* **2006**, *17*, 145.
[28] M. Nieminen, L. Niinisto, E. Rauhala, *J. Mater. Chem.* **1996**, *6*, 27.
[29] H. W. Kim, N. H. Kim, C. Lee, *J. Mater. Sci.* **2004**, *39*, 3461.
[30] N. H. Kim, H. W. Kim, C. Seoul, C. Lee, *Mater. Sci. Eng., B* **2004**, *111*, 131.
[31] S. Basharat, C. J. Carmalt, S. J. King, E. S. Peters, D. A. Tocher, *Dalton Trans.* **2004**, 3475.
[32] S. Basharat, C. J. Carmalt, R. Palgrave, S. A. Barnett, D. A. Tocher, H. O. Davies, *J. Organomet. Chem.* **2008**, *693*, 1787.
[33] C. J. Carmalt, S. J. King, *Coord. Chem. Rev.* **2006**, *250*, 682.
[34] M. Valet, D. M. Hoffman, *Chem. Mater.* **2001**, *13*, 2135.
[35] D. H. Kim, S. H. Yoo, T.-M. Chung, K.-S. An, H.-S. Yoo, Y. Kim, *Bull. Korean Chem. Soc.* **2002**, *23*, 225.
[36] L. Miinea, S. Suh, S. G. Bott, J.-R. Liu, W.-K. Chu, D. M. Hoffman, *J. Mater. Chem.* **1999**, *9*, 929.
[37] S. Basharat, W. Betchley, C. J. Carmalt, S. Barnett, D. A. Tocher, H. O. Davies, *Organometallics* **2007**, *26*, 403.
[38] S. Basharat, C. J. Carmalt, R. Binions, R. Palgrave, I. P. Parkin, *Dalton Trans.* **2008**, 591.
[39] B. Ballarin, G. A. Battiston, F. Benetollo, R. Gerbasi, M. Porchia, D. Favretto, P. Traldi, *Inorg. Chim. Acta* **1994**, *217*, 71.
[40] S. Bhattacharya, S. Singh, V. D. Gupta, *J. Chem. Crystallogr.* **2002**, *32*, 299.
[41] A. Milanov, R. Bhakta, R. Thomas, P. Ehrhart, M. Winter, R. Waser, A. Devi, *J. Mater. Chem.* **2006**, *16*, 437.
[42] A. Milanov, R. Thomas, M. Hellwig, K. Merz, H.-W. Becker, P. Ehrhart, R. A. Fischer, R. Waser, A. Devi, *Surf. Coat. Technol.* **2007**, *201*, 9109.
[43] M. Hellwig, A. Milanov, D. Barecca, J.-L. Deborde, R. Thomas, M. Winter, U. Kunze, R. A. Fischer, A. Devi, *Chem. Mater.* **2007**, *19*, 6077.
[44] A. Baunemann, M. Hellwig, A. Varade, R. K. Bhakta, M. Winter, S. A. Shivashankar, R. A. Fischer, A. Devi, *Dalton Trans.* **2006**, 3485.
[45] K. Dymock, G. J. Palenik, *Acta Crystallogr., Sect. B* **1974**, *30*, 1364.
[46] C. Djordjevic, *Spectrochim. Acta* **1961**, *17*, 448.
[47] K. E. Lawson, *Spectrochim. Acta* **1961**, *17*, 248.
[48] T. S. Lewkebandara, P. H. Sheridan, M. J. Heeg, A. L. Rheingold, C. H. Winter, *Inorg. Chem.* **1994**, *33*, 5879.
[49] O. J. Bchir, S. W. Johnston, A. C. Cuadra, T. J. Anderson, C. G. Ortiz, B. C. Brooks, D. H. Powell, L. McElwee-White, *J. Cryst. Growth* **2003**, *249*, 262.
[50] S. Pasko, L. G. Hubert-Pfalzgraf, A. Abrutis, *Mater. Lett.* **2005**, *59*, 1836.
[51] F. W. McLafferty, *Anal. Chem.* **1959**, *31*, 2072.
[52] F. W. McLafferty, R. S. Gohlke, *Anal. Chem.* **1959**, *31*, 1160.
[53] http://www.americanelements.com/gaacac.html.
[54] JCPDS-ICCD No. 41-1103.
[55] J. F. Moulder, W. F. Stickle, P. E. Sobol, K. D. Bomben, *Handbook of X-ray Photoelectron Spectroscopy* (Ed.: J. Chastain), Perkin–Elmer Cooperation, Eden Prairie, MN, **1992**.
[56] D. Briggs, M. P. Seah, *Practical Surface Analysis: Auger and X-ray Photoelectron Spectroscopy*, John Wiley & Sons, Chichester, UK, **1990**.
[57] T. Mathew, Y. Yamada, A. Ueda, H. Shioyama, T. Kobayashi, *Appl. Catal. A* **2005**, *286*, 11.
[58] http://srdata.nist.gov/xps/.
[59] T. Takeuchi, H. Ishikawa, N. Takeuchi, Y. Horikoshi, *Thin Solid Films* **2008**, *516*, 4593.
[60] 529.9–532.0 eV in: http://srdata.nist.gov/xps/.
[61] A. Devi, W. Rogge, A. Wohlfart, F. Hipler, H. W. Becker, R. A. Fischer, *Chem. Vap. Deposition* **2000**, *6*, 245.

Received: October 30, 2008
Published Online: February 3, 2009

